THE
PHYSICAL REVIEW

A journal of experimental and theoretical physics established by E. L. Nichols in 1893

SECOND SERIES, VOL. 166, NO. 4 20 FEBRUARY 1968

M/L Orbital-Electron-Capture Ratio in Ar^{37} Decay and the Fraction of K_α X Rays in the K Series of Chlorine*

J. P. RENIER, H. GENZ, K. W. D. LEDINGHAM,† AND R. W. FINK
School of Chemistry, Georgia Institute of Technology, Atlanta, Georgia
(Received 8 September 1967)

The ratio of M- to L-orbital electron capture in the decay of 35-day Ar^{37} has been measured in a single-wire proportional counter containing the gaseous source. This counter was operated with variable paralysis times, 2.0 and 3.8 msec being used in the present experiments to minimize the contribution from afterpulses. Recent investigations of the pulse-height distribution from proportional counters due to single- and multiple-electron events make it possible to measure single-electron spectra down to essentially zero energy with much greater accuracy than heretofore. The experiment was undertaken because of the considerable disagreement between experimental and theoretical M/L capture ratios, particularly in the low-Z region. A survey of all experimental work on M capture is included for comparison with available theoretical results. In the decay of Ar^{37} the experimental value for the M/L capture ratio is $P_M/P_L=0.104_{-0.003}{}^{+0.006}$, where the error limits have been subjected to careful detailed analysis. From this result, a value of $k_\alpha=0.980\pm0.015$ for chlorine was determined, where k_α is the fraction of K_α x rays in the K series of chlorine. The theoretical predictions of Bahcall for P_M/P_L lie about 23% above the experimental point, for a theory with exchange correction. The older theoretical value due to Wapstra *et al.* is in no better agreement with experiment, even if a correction for exhange is applied. An intensive effort is reported to measure the L/K capture ratio in the decay of 53.5-day Be^7, as gaseous $(C_2H_5)_2Be^7$ in the single-wire proportional counter, but owing to the low energy of the K-capture events (55 eV) and very low counting statistics, this measurement appears to be beyond the present state of the proportional-counter art.

INTRODUCTION

EXPERIMENTAL $|M_I/L_I|^2$ wave-function ratios derived from allowed M/L orbital-electron-capture ratios are compared[1] in Fig. 1 with the three existing theoretical curves. Curve A was calculated by Wapstra and Van der Eijk,[2] using Slater screening constants in hydrogenlike wave functions. Curves C and B, respectively, in the region $13\leqslant Z\leqslant 37$ were calculated by Bahcall[3] with and without correction for electron-exchange–atomic overlap. In the region of $55\leqslant Z\leqslant 90$, curves C and B, respectively, are due to calculations by Robinson[4] with and without an extrapolated Bahcall correction. The regions between $Z=37$ and $Z=55$ in curves B and C were obtained by smooth interpolation.

The experimental points in Fig. 1 are those obtained with proportional counters containing gaseous radioactive sources, except for point g for Cd^{109}, point j for Tl^{202g}, and point m for Os^{185}.

It may be seen from Fig. 1 that curves B and C, based on the more refined wave functions used by Bahcall[3] and Robinson,[4] lie systematically above the experimental points. The inset in Fig. 1 shows the previous result[5] for the Ar^{37} M/L ratio, together with the theoretical curves. The error limits on this point are too large to determine which theory agrees best with the experiment. In the low-Z region, the differences between the three theoretical curves are greatest, and, moreover, Ar^{37} is the most suitable experimental case for investigation. The large error limits in the previous Ar^{37} experiment[5] arose chiefly from an inability to separate unambiguously the M and L spectra, because of uncertainties in spectral shapes produced in proportional counters by events having energies below about 300 eV.

* Supported in part by the U. S. Atomic Energy Commission.
† Present address: Department of Natural Philosophy, University of Glasgow, Glasgow, Scotland.
[1] R. W. Fink and K. W. D. Ledingham, Bull. Am. Phys. Soc. **11**, 352 (1966).
[2] A. H. Wapstra and W. Van der Eijk, Nucl. Phys. 4, 325 (1957); A. H. Wapstra, G. J. Nijgh, and R. Van Lieshout, *Nuclear Spectroscopy Tables* (North-Holland Publishing Co., Amsterdam, 1959), p. 61.
[3] J. N. Bahcall, Phys. Rev. **131**, 1756 (1963).
[4] B. L. Robinson, Nucl. Phys. **64**, 197 (1965).
[5] P. W. Dougan, K. W. D. Ledingham, and R. W. P. Drever, Phil. Mag. **7**, 475 (1962).

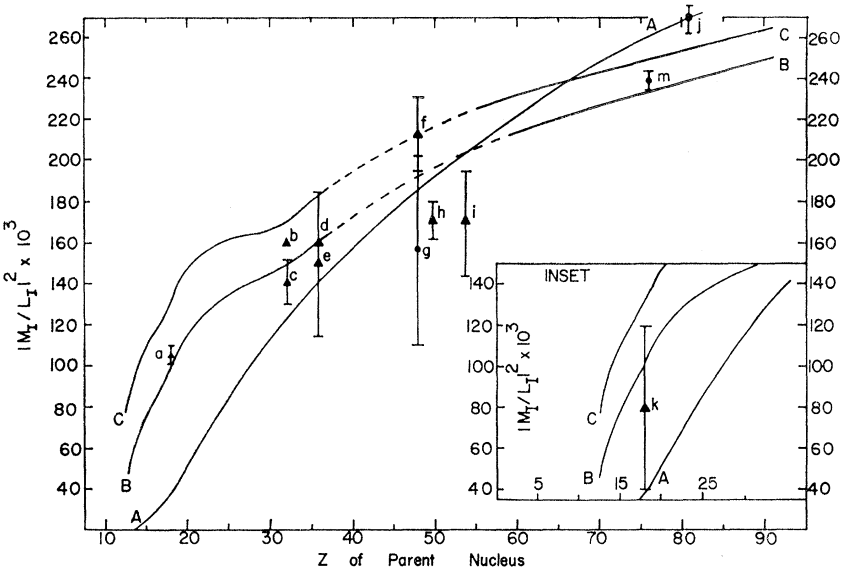

FIG. 1. Comparison of experimental M/L orbital-electron-capture ratios with theoretical results. Inset: The region near $Z=18$ with the previous result for Ar^{37} from Ref. 5. Curve A-A is the theoretical estimate of Wapstra *et al.*, Ref. 2, based on hydrogenlike wave functions with Slater screening. No correction for electron-exchange atomic overlap is included. Curve B-B is the region $Z=13$ to 37 is the theoretical result of Bahcall, Ref. 3, based on Hartree-Fock wave functions calculated by Watson and Freeman, and in the region $Z=55$ to 90 is the theoretical result of Robinson, Ref. 4, based on M-shell wave functions of Brewer, Harmer, and Hay. The region $Z=37$ to 55 is a smooth interpolation between the results of Bahcall and those of Robinson. No correction for electron-exchange atomic overlap is included. Curve C-C is the same as B-B, except that the electron-exchange–atomic-overlap correction calculated by Bahcall, Ref. 3, has been applied between $Z=13$ and 37. This correction has been *extrapolated* in the region of $Z\geq 37$. ▲ indicates points from direct experimental measurements of the M/L capture ratio with gaseous internal sources in single- or multiwire proportional counters. ● indicates all other values of M/L capture ratios derived from precision measurements of $(L+M+N+\cdots)/K$ ratios, with values of the L/K capture ratio taken either from a precision experimental measurement or from exchange-corrected theory in cases where an accurate value of Q_{EC} is known from independent measurements.

The experimental points are as follows: (a) Ar^{37}, $M/L=0.104_{-0.003}{}^{+0.006}$ [present investigation] ($Q_{EC}=815\pm5$ keV); (b) Ge^{71}, $M/L=0.16\pm0.08$ [P. W. Dougan and R. W. P. Drever, unpublished studies, 1959, quoted in P. W. Dougan, thesis, 1963 (unpublished)] ($Q_{EC}=237\pm5$ keV); (c) Ge^{71}, $M/L=0.141\pm0.010$ [C. Manduchi and G. Zannoni, Nuovo Cimento **24**, 181 (1962); Nucl. Phys. **36**, 497 (1962)] ($Q_{EC}=231\pm3$ keV); (d) Kr^{79}, $M/L=0.16\pm0.08$ [P. W. Dougan and R. W. P. Drever, unpublished studies, 1959, quoted in P. W. Dougan, thesis, 1961 (unpublished)]; (e) Kr^{79}, $M/L=0.150\pm0.035$ [G. Winter (private communication, 1966)]; (f) Cd^{109}, $M/L=0.232\pm0.020$ [R. B. Moler and R. W. Fink, Phys. Rev. **139**, B282 (1965)]; note: since $Q_{EC}=80_{-3}{}^{+7}$ keV to the 88-keV, 40-sec Ag^{109m} state, $q=(80-0.775)^2/(80-4.02)^2=1.087$, whence $|M_I/L_I|^2=(0.232\pm0.020)/1.087=0.213\pm0.018$, which is plotted; (g) Cd^{109}, $(M+N+)/L=0.170\pm0.05$, from experiments with NaI(Tl) crystals containing Cd^{109}. [H. Leutz, K. Schneckenberger, and H. Wenninger, Nucl. Phys. **63**, 263 (1965)], and using $q=1.087$, a value of $|M_I/L_I|^2=0.156\pm0.05$ is plotted; (h) Sn^{113}, $M/L=0.20\pm0.01$ [C. Manduchi, G. Nardelli, M. T. Russo-Manduchi, and G. Zannoni, Nuovo Cimento **33**, 49 (1964); **31**, 1380 (1964)]. Since $Q_{EC}=49\pm3$ keV to the 393-keV level, $q=(49-0.868)^2/(49-4.445)^2=1.167$, from which $|M_I/L_I|^2=(0.20\pm0.01)/1.167=0.171_4\pm0.01$ is plotted; (i) Xe^{127g}, $M/L=0.185\pm0.025$ [G. Winter (private communication, 1966); G. Winter, K. Hohmuth, and J. Schintlmeister, Nucl. Phys. **73**, 91 (1965)]; (j) Tl^{202g}, $M/L=0.269\pm0.007$, to the 440-keV level in Hg^{202}, from crystals of NaI(Tl) containing Tl^{202g} [H. Leutz, G. Schulz, and H. Wenninger, Nucl. Phys. **75**, 81 (1965)]. $Q_{EC}=797$ keV to the 440-keV level. This transition is first-forbidden unique, and, in a strict sense, it cannot be compared rigorously with theory for allowed transitions. However, the difference may be smaller than the experimental and theoretical errors. For this reason, the location of the point for Tl^{202g} is interesting; (m) Os^{185}, $M/L=0.254\pm0.005$, to the 646-keV level in Re^{185}, from crystals of NaI(Tl) containing Os^{185}. [G. Schulz, Nucl. Phys. **A101**, 177 (1967)]. The point plotted, corrected for the neutrino energies, is $|M_I/L_I|^2=0.239\pm0.005$.

Recent investigations[6–11] of the pulse-height distributions from proportional counters due to single- and multiple-electron events make it possible to repeat the Ar^{37} M/L capture measurement with much greater accuracy.

EXPERIMENTAL

Several Ar^{37} sources were prepared by irradiations of natural argon in the Georgia Tech reactor. The sources were contained under pressure in a vessel filled with Na-Pb alloy[12] to assure long-term freedom from possible atmospheric contamination. From the spectra obtained, it is evident that radioactive contamination by Ar^{39}, Ar^{41}, or other activities was negligible.

A small single-wire aluminum proportional counter having a sensitive length of 20 cm and an inner diameter of 4.17 cm was used. This was fitted with earthed guard tubes and with field tubes. An external window of 0.65

[6] A. P. Lukirskii, O. A. Ershov, and I. A. Brytov, Bull. Acad. Sci. USSR, Phys. Ser. **27**, 447 (1963); **27**, 798 (1963).

[7] R. Gold and E. F. Bennett, Phys. Rev. **147**, 201 (1966).

[8] J. L. Campbell and K. W. D. Ledingham, Brit. J. Appl. Phys. **17**, 769 (1966).

[9] P. J. Campion and D. K. Murray, Intern. J. Appl. Radiation and Isotopes **18**, 203 (1967).

[10] J. H. Carver and P. Mitchell, Nucl. Instr. Methods **52**, 130 (1967).

[11] H. Schlumbohm, Z. Physik **152**, 49 (1958).

[12] Kindly donated by the Ethyl Corp., Baton Rouge, La.

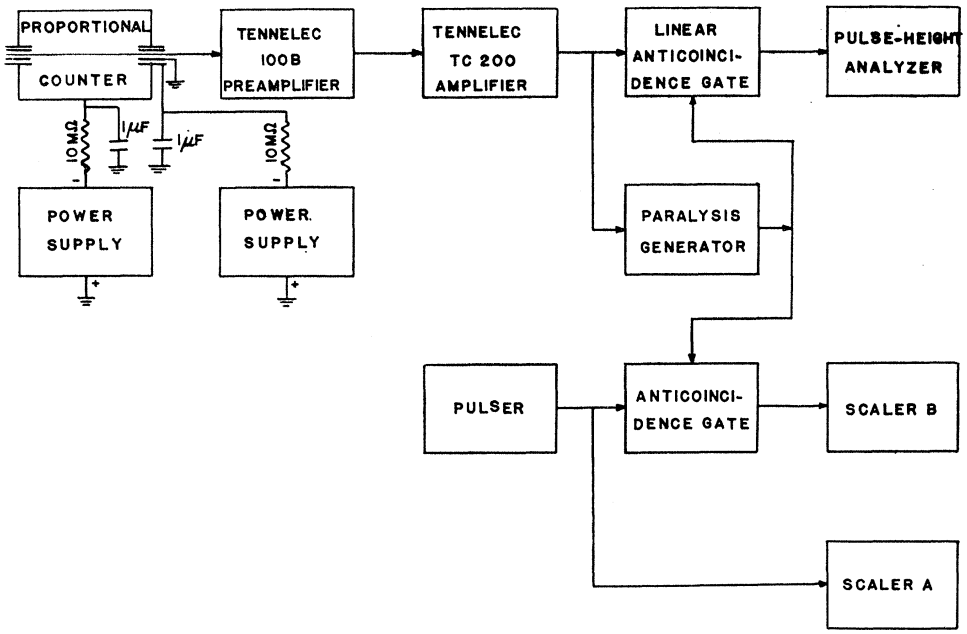

FIG. 2. Block diagram of the single-wire proportional-counter electronic system.

cm diam. was provided which could be used either with Mylar (40 mg/cm^2) or with a 23.5-mg/cm^2 beryllium window to admit either external ultraviolet photons or x rays, respectively, for calibration. The center wire was of 0.0075-cm-diam. stainless steel. The counter was operated with negative high voltages on the case and field tubes and was shielded by 5 cm of lead.

The gas filling consisted of argon with 15% propane admixed, after evacuation to 10^{-5} Torr. The only difference observed with ordinary high-purity tank argon and ultra-high-purity argon having less than 10 ppm total impurities, with the actual gas analysis supplied by the manufacturer, was that the initial resolution was maintained for a longer time with the latter. Mixtures of argon-methane and argon-acetylene also were investigated, but the best resolution was obtained with argon-propane. Runs were made with pressures from 0.5 to 3 atm, in order to vary the K x-ray escape, which is a critical correction factor as shown below.

In Fig. 2 the block diagram of the electronic circuitry is shown. Negative high voltages for the field tubes and cathode of the counter were obtained from two separate Fluke power supplies. The use of negative high voltage on the outer case of the counter is superior to grounding of the case with positive high voltage on the center wire, because a coupling capacitor between the center wire and the first stage of the preamplifier, with its problems of leakage and spurious discharges, is then eliminated. The cathode was typically operated between negative 2000 and 4000 V, depending on the filling pressure. RC filters, shown in Fig. 2, were used for smoothing the ripple due to the power supply and to the charge-collection rate in the counter. The field-tube voltage was calculated from the dimensions of the counter to be about 60% of the outer case voltage; however, the optimum resolution for the 2.82-keV K peak in Ar^{37} decay was obtained experimentally with a field-tube voltage of 72%. Even slight deviations ($\pm 5\%$) from the optimum field-tube voltage caused obvious asymmetries in the shape of the K peak. The influence of the precise centering of the anode wire inside the guard tubes within the field tubes was found to be extremely critical for good resolution and for high peak-to-valley ratios between the K and L and between the L and M regions of the spectrum.

The center wire of the counter was dc-connected to the grid of the first tube (selected Amperex 6922) of a Tennelec 100B preamplifier, the output of which was fed into a Tennelec TC-200 amplifier, which was operated in a doubly differentiated mode with time constants typically of the order of 1.6 μsec. These pulses were fed via a linear anticoincidence gate, modified for zero-time recovery, into a Nuclear Data 128-channel analyzer. The gating pulse was triggered at the zero crossover point of the pulse to be analyzed. The gate was controlled by pulses generated by a paralysis pulse generator. The transistorized paralysis pulse generator[13,14] was constructed to eliminate the small after-

[13] R. W. P. Drever kindly furnished tube-type circuits for the paralysis pulse generator from which the transistorized version was designed (private communication).

[14] Circuit diagrams for the transistorized paralysis pulse generator and for the modified linear anticoincidence gate are contained in the M.S. thesis of J. P. Renier, Georgia Institute of Technology, 1967, available as U. S. Atomic Energy Commission Report No. ORO-3346-10, 1967 (unpublished).

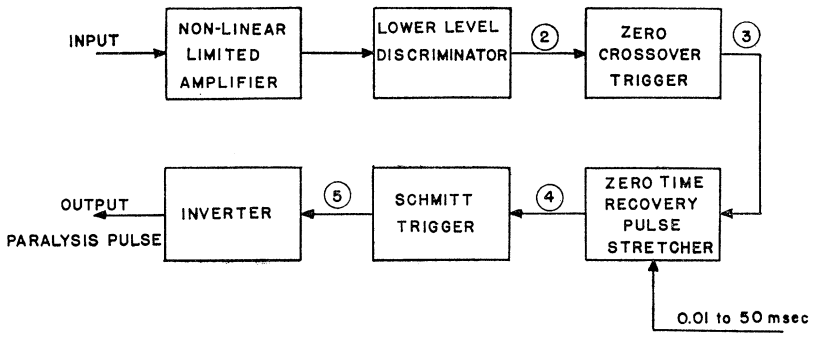

FIG. 3. Block diagram of the paralysis pulse generator.

pulses which follow large pulses[5,15] (see discussion of afterpulses below). A block diagram of the paralysis pulse generator is shown in Fig. 3.

The paralysis pulse generator was constructed to have zero-time recovery,[14] and it produced gating pulses of width variable from zero to 50 msec. The zero-time recovery feature means that a pulse, (whether due to background, K, L, or M events) that arrives at a time during which the modified linear anticoincidence gate (Sturrup Model 1450) is closed by a paralysis pulse, triggers an additional paralysis pulse which continues to keep the gate closed in order to prevent detection of possible afterpulses. The triggering level of the paralysis pulse generator was set high enough to avoid triggering by noise. The sequence of pulses through the paralysis pulse generator is shown in Fig. 4.

A modification of the linear anticoincidence gate (Sturrup Model 1450) was necessary, because the gate driver of the gate did not have zero-time recovery. The paralysis gating pulse from the paralysis pulse generator was fed to a suitable point in the gate driver circuit of the gate (see Ref. 14). By this means, zero-time recovery was accomplished in the linear anticoincidence gate.

To measure the effective open time of the linear anticoincidence gate, a second anticoincidence gate, also modified to have zero-time recovery,[14] was operated in parallel with the first one. The paralysis pulse triggered both gates simultaneously. The signal input of the second gate was fed by a pulser. Scaler A, connected to the pulser, and scaler B (see Fig. 2), connected to the output of the second gate, determined the ratio of open/total time.

The stability of the experimental system as determined by the channel shift of a calibration peak typically was less than 1% in 24 h.

When the energy of a capture event is lower than that required to produce an ion pair (about 26.5 eV in argon-propane), the primary single electron triggers an avalanche whose pulse-height distribution in the proportional region has been carefully investigated[6–11] and found to be dependent on experimental conditions, such as gas gain, type of filling gas, and pressure. Contrary to earlier thinking,[16] the single-electron spectrum cannot

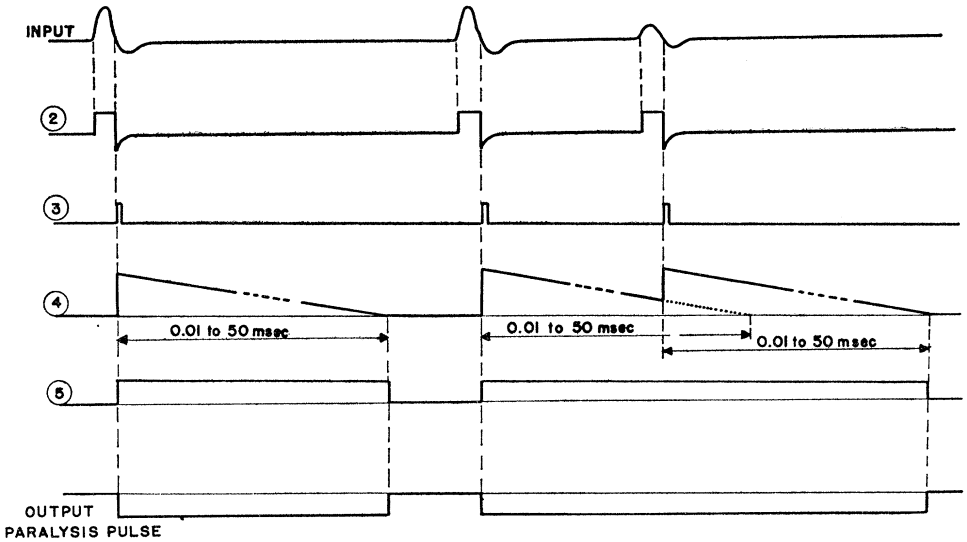

FIG. 4. Pulse time sequence of the paralysis pulse generator.

[15] P. W. Dougan, K. W. D. Ledingham, and R. W. P. Drever, Phil. Mag. 7, 1223 (1962).
[16] H. S. Snyder, Phys. Rev. 72, 181 (1947); O. R. Frisch, Atomic Energy of Canada, Ltd. Report No. CRL-57, 1959 (unpublished).

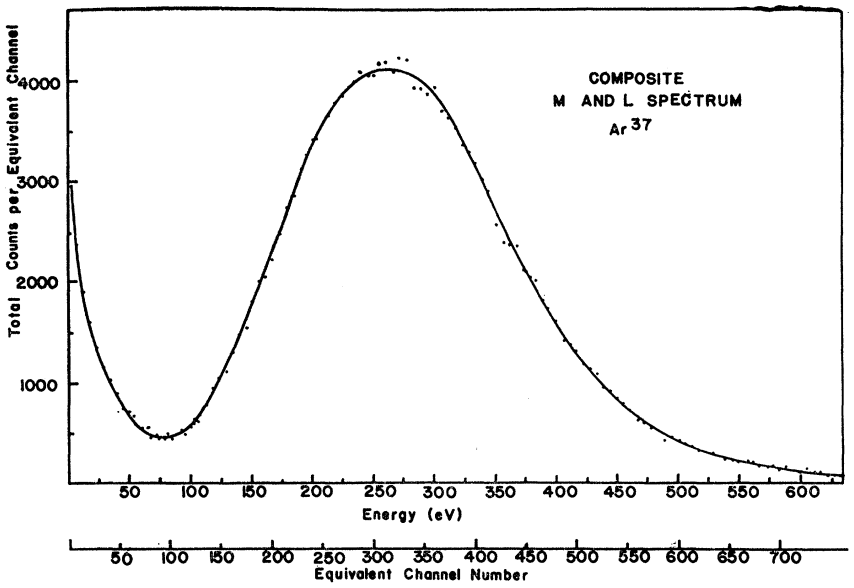

FIG. 5. The observed normalized M and L spectrum from Ar^{37} decay, after correction for dead time and subtraction of background.

be represented by an exponential function (e^{-x}), nor by a quasiexponential function ($x^{1/2}e^{-x}$).[17] Therefore, in order to know the exact single-electron spectrum for a given experimental system, it is necessary to determine the single-electron spectrum experimentally.[6–11]

Accordingly, single electrons were generated in the counter by introducing ultraviolet photons from an incandescent uv bulb through the 40 mg/cm² Mylar window, producing photoelectrons from the aluminum wall. These photoelectrons have maximum energies of only a few eV.

In the Ar^{37} experiments, the spectral shape of single electrons was determined for each Ar^{37} M-capture spectral measurement (see below).

In the M region (see Figs. 5 and 6), some of the pulses arise from causes other than M capture. For example, small pulses can be created by the clipping of large pulses due to the electronic system, and this effect became increasingly evident at counting rates above 300 dis/sec. Radiative electrical pickup also can induce small pulses in the system. Possible negative-ion formation from electron attachment from large pulses in the counter gas also is manifested by small afterpulses.[5,15] Although the paralysis unit is designed to eliminate these small afterpulses, *it cannot eliminate a true primary M-capture event*, which immediately forms a negative ion by attachment during the open time of the gate.

When the paralysis pulse generator was disconnected, small afterpulses in the Ar^{37} experiments were observed in the energy region below about 100 eV. Most of these afterpulses had time delays of less than about 700 μsec. These afterpulses have been reported previously in Ar^{37} and Cl^{36} studies in proportional counters.[5,15] Afterpulses up to 400-μsec delays have been found in Geiger-Müller counters as well.[18]

The origin of afterpulses is not completely understood at present. Several possible mechanisms giving rise to afterpulses have been suggested. One of these is electron attachment leading to negative-ion formation, following the primary ionizing event. Owing to the fact that negative ions are created throughout the sensitive

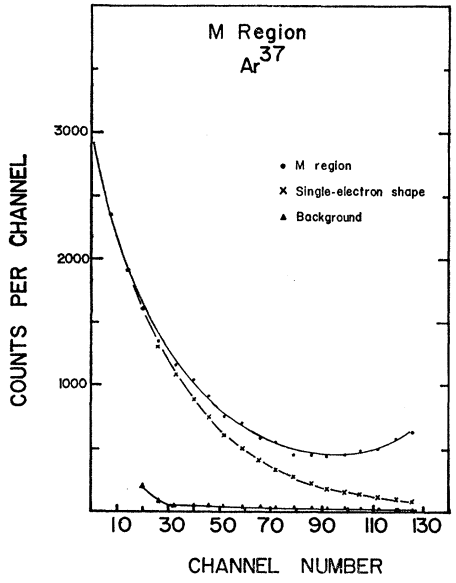

FIG. 6. The M region due to Ar^{37} decay, together with the single-electron spectrum due to introduction of ultraviolet photons from an external source under identical conditions. The single-electron spectrum has been normalized to the M spectrum. Details of the fitting of the single-electron to the M spectrum are discussed in the text.

[17] S. C. Curran, A. L. Cockcroft, and J. Angus, Phil. Mag. **40**, 929 (1949).

[18] H. Weiss and E. Masanz, Atomkernenergie **11**, 489 (1966).

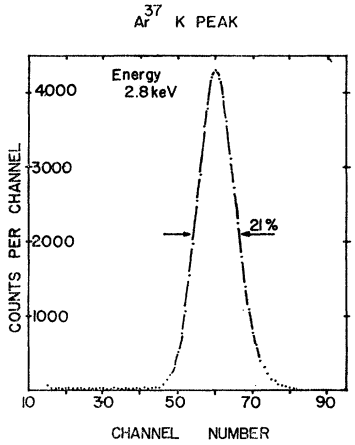

FIG. 7. The K peak due to Ar^{37} decay. The low-energy tail from degraded K events must be taken into account in the L and M regions, as discussed in the text.

volume of the counter, they will exhibit a variety of transit times for collection on the anode center wire, depending on the size of the counter and on the molecular weight and charge of the negative ion. If this mechanism is present, the afterpulses will depend on the concentration of oxygen, moisture, or any other electronegative impurities present (or introduced for investigative purposes). Another mechanism can be termed the "positive-ion echo effect." Since most of the positive ions are created in the electron avalanche which occurs within a few wire diameters of the center wire, they travel as a bunch towards the cylindrical cathode walls, and their transit time for charge collection is relatively constant. When the positive-ion bunch arrives at the cathode wall, it causes emission of a secondary-electron bunch, which then travels back to the center wire with essentially constant transit time, where it initiates another avalanche with formation of another positive-ion bunch, which repeats the process. This "echo effect" is repeated with diminishing intensity at constant time intervals.

These two mechanisms for formation of afterpulses lead to two very different time distributions of afterpulses following a primary ionization event. Therefore, an investigation of the time distribution of afterpulses in proportional counters may enable us to distinguish the process chiefly responsible.[19]

In the present investigation, total counting rates were limited to 110 dis/sec, in order to minimize the clipping effect. Electrical pickup was minimized by careful electrostatic screening and grounding.

In order to determine the optimum paralysis time necessary to eliminate afterpulses, a series of runs was done in which M spectra of Ar^{37} were compared as a function of paralysis pulse width from zero to 8.5 msec. No significant difference in the spectrum was observed with paralysis times longer than about 700 μsec with a fresh Ar^{37} source (less than 2 months after the end of reactor irradiation).[14] As the source aged (up to 6 months after irradiation, with storage over Na-Pb alloy at room temperature), a gradual increase in this minimum paralysis time was found to be necessary, up to about 2 msec. This suggests that the concentration of electron-attaching impurities (oxygen, moisture) gradually increased as the source aged, in spite of the presence of Na-Pb alloy. Therefore, all further experiments on Ar^{37} were run with paralysis times of 2.0 and 3.8 msec, depending on the age of the source, in order to assure that the M spectrum was independent of effects due to negative-ion formation and afterpulses.

The counter was operated at gas gains up to 10^4, well within the range of proportionality.[20] With this gas gain, the mean pulse height of single electrons was approximately 10 times greater than noise. In order to get good linear response from a proportional counter, the quantity mE should be kept below a value of 10^8, where m is the gas gain and E is the energy of the primary ionizing event in eV.[20] An external source of 2.9-yr Fe^{55} was used as a calibration standard (K_α x rays $=5.9$ keV). When the gas gain is set at about $m=10^4$, then the quantity mE is 2.8×10^7 for the Ar^{37} K peak (2.82 keV) and is 5.9×10^7 for the K_α x rays of Fe^{55}. Thus, in order to keep mE for the Fe^{55} standard within the prescribed limit, the gas gain was kept below 10^4. The resolution of the Fe^{55} K_α x rays typically was $(16\pm1)\%$ full width at half maximum (FWHM). The Ar^{37} K peak at 2822 eV was observed periodically throughout the runs to check counter resolution at this energy [$(21\pm1)\%$ FWHM], as shown in Fig. 7, to check gain stability (which typically was $\frac{1}{2}$ channel per 24 h), and for the purpose of determining the L/K intensity ratio, a quantity required in the evaluation of the results.

The linearity of the system, including the 128-channel analyzer, was carefully measured with a mercury pulser. This linearity measurement is important for the fitting of the M to the L spectrum, which must be measured in separate runs, and also for the fitting of the single-electron spectrum in the M region, as explained below.

The discrimination level of the paralysis pulse generator was set at a level corresponding to about 10 eV in the M region. Many electronic checks such as the determination of the analyzer zero-point and nonlinearity, of the discrimination levels for the analyzer and the paralysis pulse generator, of the pedestal of the linear anticoincidence gate, and of gain stability, were made before and after each run.

The M, L, and K spectra were taken in separate runs at the *same* gas gain ($\approx10^4$) but with *different* relative electronic gains of 64, 8, and 1.0, respectively. The total

[19] Such a time-distribution experiment by H. Genz, D. S. Harmer, and R. W. Fink, using a two-parameter analyzer for energy and time analysis of proportional-counter pulses has been performed [Nucl. Instr. Methods (to be published)].

[20] G. C. Hanna, D. H. W. Kirkwood, and B. Pontecorvo, Phys. Rev. 75, 985 (1949).

gain per primary electron was not kept constant, but was adjusted for the L and M spectra, in order to make the upper part of the M spectrum overlap the lower part of the equivalent L spectrum, and thus to fit the two spectra into a composite one for measurement of the M/L intensity ratio (see Fig. 5). (The M, L, and K spectra must be taken separately, in order to expand each of these regions of interest over the limited 10 V range of the ADC of the analyzer.) To obtain reasonable statistics, runs in the M region and L regions normally took up to 15 and 6 h, respectively.

Background was determined by refilling the counter with the same gas mixture, but omitting Ar^{37}. The external Fe^{55} source was used to recalibrate for identical gas gain. The background runs normally were of the same duration as the source runs. The mean intensity of the background in the M region (see Fig. 6) was less than 1 count/channel/h. Data from the runs were printed out and also were stored on Tally paper tape for subsequent analysis by computer.

More than 30 runs were performed at various pressures, paralysis times, amplification gains, counting rates, and with two different Ar^{37} sources. The results of these runs are summarized in Table I.

RESULTS OF MEASUREMENTS

Data and Computation of Observed Intensity Ratios N_L/N_K and N_M/N_L

From a precise knowledge of the gain ratio between the M and L spectra, the two spectra were fitted together by means of a computer program[21,22] into a composite spectrum (Fig. 5) having equalized channel widths for the M and L regions. A check on the goodness of the fit in the region of overlap between the M and L spectra was obtained from the fact that the intensities of the M points and of the L points matched in the overlap region.

To separate the contributions from M and L events in the region of overlap, the single-electron spectrum (from ultraviolet photons) was fitted in the M region by the computer program.[22] This program was developed for the complete analysis of these experiments.[22] In sequence, this program performs the following operations on the M, L, K, single-electron, and background spectra, respectively: (1) dead-time correction and normalization to unit clocktime; (2) nonlinearity correction in the lower channels; (3) background subtraction; (4) normalization to equivalent channels for L and K spectra to the M-spectrum channel width, which gives an M-, L-, and K-composite spectrum; (5) subtraction of the contribution in the M and L regions from degraded K events (discussed below); (6) fitting of the single-electron spectrum in the M spectral region (discussed below); (7) extrapolation to zero energy; (8) calculation of net M, L, and K events and of N_M/N_L and N_L/N_K ratios; and (9) determination of the orbital-electron-capture ratio P_M/P_L as a function of k_α, the fraction of K_α x rays in the K-x-ray series of chlorine (discussed below).

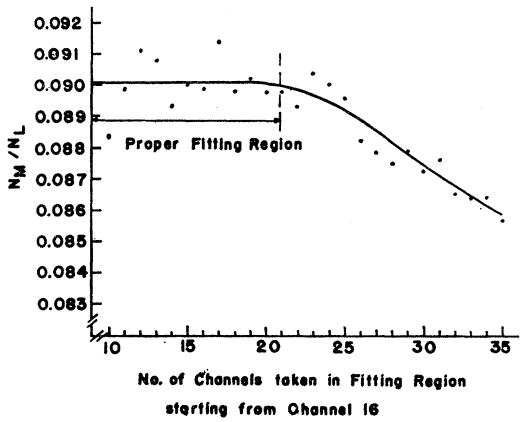

FIG. 8. A typical plot of the intensity ratio N_M/N_L versus successive fits of the single-electron to the M spectrum. The decrease in the N_M/N_L ratio with larger fitting regions in the M spectrum reflects the increasing contribution of L capture events. Therefore, the correct fitting region is the horizontal portion before this decrease sets in.

After subtraction of background, the region between the K peak (2822 eV) and the L peak (265±10 eV) exhibits a constant residual intensity, probably arising from degradation of some K events in the counter.[23,24] This low-energy tail from the K peak has been extrapolated horizontally to zero energy.[24] It contributes an uncertainty in the final M/L intensity ratio of about 5% (computer operation No. 5 above).

In order to fit the single-electron spectrum in the M region, computer operation No. 6 first converts the two spectra to logarithmic form, since it has been shown by Gold and Bennett[7] that this energy region (5 to 20 eV) is well approximated by an exponential function at gas gains in the region of 10^4. A least-squares fit to a straight line is then done on the logarithmic forms of the single-electron spectrum and the M spectrum. This fitting to a straight line is repeated from the lowest energy successively to higher and higher energies in the M region. Each of these successive fittings of the M spectrum to a straight line in the logarithmic plot results in a *new line* of decreasing slope. Each such single-electron fit is then

[21] All computations were carried out with the Georgia Tech Burroughs 5500 computer.

[22] J. P. Renier, computer program (to be published).

[23] W. Heuer, Z. Physik **194**, 224 (1966).

[24] The degradation of a very small fraction of the total K events is thought to arise from secondary electrons ejected from the aluminum wall when K x rays strike it, and also from K x rays which escape *in part* from the sensitive volume into the insensitive end zones of the counter, where the field tubes cut off the gas multiplication, or from the end zones into the sensitive volume. Another possible contribution to the degradation arises from possible losses of optical photons from the electron avalanche. Such photons do not produce single electrons and so constitute an uncompensated energy loss. These degradation effects appear to give rise to a constant-intensity energy distribution below the K peak.

normalized to the M spectrum at the lowest-energy point, and a linear extrapolation in the logarithmic form of the single-electron spectrum is performed back to zero energy. This extrapolation to zero energy meets the criterion of Gold and Bennett[7] for the proper definition of a given single-electron spectrum. The entire procedure determines the variation of the N_M/N_L intensity ratio with successive fits of the single-electron spectrum to the M spectrum. This is plotted in Fig. 8. The significance of Fig. 8 is that it defines the proper region of the M spectrum to be fitted by the single-electron spectrum, where the contribution from L-capture events is negligible. The decrease in the N_M/N_L ratio with larger fitting regions in the M spectrum in Fig. 8 reflects the increasing contribution of L events. The proper fitting region is therefore the horizontal portion before this decrease due to L events sets in.

Correction for K-X-ray Escape and Calculation of Final Results

The values obtained, Table I, for N_L/N_K and N_M/N_L intensity ratios must be corrected for K-x-ray escape for the following reason. When a K_α x ray escapes detection *entirely*, the primary K-shell vacancy appears in the L shell, and the event will be registered in the L peak; similarly, when a K_β x ray escapes, the primary K vacancy appears in the M shell, and the event will be registered in the M spectrum. The detection efficiency is essentially 100% for L and M x rays and Auger electrons; thus in these experiments, the escape of L and M events is taken to be zero.

Owing to the fact that there are some 10 times more K captures than L captures, and some 10 times more L captures than M captures, even a small fraction of K-x-ray escape gives rise to an appreciable correction in the L and M intensities. This correction, in turn, depends critically on the value of the K fluorescence yield[25] ω_K of the daughter atom, chlorine, and on the probability P for escape of K x rays without detection from the counter.[26]

The results were calculated by means of the following quantitative relationships. The observed number of events in the M spectrum is given by

$$N_M=P_M+(\omega_K P)P_K k_\beta \tag{1}$$

and the observed number of events in the L peak is given by

$$N_L=P_L+(\omega_K P)P_K k_\alpha. \tag{2}$$

The observed number of events in the K peak is

$$N_K=P_K-(\omega_K P)P_K(k_\alpha+k_\beta), \tag{3}$$

where $k_\alpha+k_\beta=1$, k_α=fraction of K_α x rays in the K-x-ray series for the daughter atom (chlorine, $Z=17$), k_β=fraction of K_β x rays in the K-x-ray series for the daughter atom, and P_M, P_L, and P_K are the respective probabilities of orbital-electron capture from the M, L, and K shells occurring in the sensitive volume of the counter. The above equations are based on the assumption that no escape of K Auger electrons or of L or M events occurs. The only escape is due to K x rays. From the above equations, one obtains

$$(\omega_K P)=[(N_L/N_K)-(P_L/P_K)]/[(N_L/N_K)+k_\alpha], \tag{4}$$

which is the fraction of K x rays escaping detection entirely. The orbital-electron-capture ratio P_M/P_L is then given by

$$(P_M/P_L)=(N_M/N_L)\left[1+\frac{(\omega_K P)k_\alpha}{(P_L/P_K)}-\frac{(\omega_K P)k_\beta}{(P_L/P_K)(N_M/N_L)}\right], \tag{5}$$

where the quantity $(\omega_K P)$, the fraction of K-x-ray escape, is obtained from Eq. (4) as a function of k_α, from the experimental measurement of the N_L/N_K ratio and a value of $P_L/P_K=0.102\pm0.003$ from the precision measurements summarized in the literature.[27] The final values of the orbital-electron-capture ratio P_M/P_L are computed from Eq. (5) by means of the computer program described above.[22]

A typical numerical evaluation of Eq. (5) for runs at 1 atm pressure gives

$$P_M/P_L=0.078+0.481[(1.078k_\alpha-1)/(k_\alpha+0.151)]. \tag{6}$$

From Eq. (6) it can be seen that the corrected capture ratio P_M/P_L is a sensitive function of k_α for single-wire proportional-counter experiments having substantial escape of K x rays. In this example, P_M/P_L varies by about 95%, from 0.048 to 0.1110 as k_α varies by only about 13%, from 0.87 to 1.00. The value of P_M/P_L is expressed in Eqs. (5) and (6) in terms of k_α, because below $Z=23$, no values of k_α are known.[28,29]

Since P_M/P_L in Eqs. (5) and (6) is sensitive to the unknown value of k_α, runs at various pressures from 0.5 to 3.0 atm were carried out, in order to vary significantly the K-x-ray escape probability $(\omega_K P)$. By this means the values of P_M/P_L in Ar^{37} decay and of k_α for chlorine ($Z=17$) were determined in the present experiments.

In the literature value[27] of $P_L/P_K=0.102\pm0.003$ used in the present calculations, various values of k_α (from 0.87 up) were employed by various authors to

[25] R. W. Fink, R. C. Jopson, Hans Mark, and C. D. Swift, Rev. Mod. Phys. 38, 513 (1966).

[26] B. L. Robinson and R. W. Fink, Rev. Mod. Phys. 27, 424 (1955); 32, 117 (1960).

[27] R. W. Fink, U. S. Atomic Energy Commission Report No. ORO-3346-8 (Rev.), 1966; Nucl. Phys. (to be published).

[28] J. H. Williams, Phys. Rev. 44, 146 (1933) and H. T. Meyers, Wiss. Verh. Siemens Labor. 7, 108 (1929), as summarized by A. H. Wapstra, G. J. Nijgh, and R. Van Lieshout, *Nuclear Spectroscopy Tables* (North-Holland Publishing Co., Amsterdam, 1959), p. 81.

[29] S. I. Salem and J. P. Johnson, Bull. Am. Phys. Soc. 11, 914 (1966).

TABLE I. Summary of results of experimental runs.[a]

Pressure	0.5 atm		1 atm		2 atm		3 atm	
Intensity ratios	N_M/N_L	N_L/N_K	N_M/N_L	N_L/N_K	N_M/N_L	N_L/N_K	N_M/N_L	N_L/N_K
	0 074	0.170	0.076	0.152	0.090	0.130	0.092	0.118
	0.073	0.171	0.078	0.154	0.090	0.127	0.095	0.117
	0.075	0.172	0.078	0.149	0.090	0.128	0.095	0.116
	0.072	0.172	0.079	0.151	0.090	0.128	0.093	0.117
	0.071	0.171	0.076	0.150	0.089	0.128		
			0.079	0.148				
Mean values	0.073	0.171	0.078	0.151	0.090	0.128	0.094	0.117

[a] Error limits (see text) on values of N_M/N_L are $(_{-3}{}^{+5.5})\%$, and on values of N_L/N_K are $\pm 1\%$.

correct for K-x-ray escape in the multiwire counter measurements. Since the K-x-ray escape probability, however, is only of the order of 10^{-4} to 10^{-5} in multiwire proportional counters having a wall-less anticoincidence ring, the value of P_L/P_K has a negligible dependence on k_α.

Table I gives a summary of observed intensity ratios N_M/N_L and N_L/N_K in the runs performed at the various pressures. A complete computer calculation was carried out for each run to obtain these ratios. The mean value at each pressure was then used to compute from Eq. (5) the dependence of P_M/P_L on k_α, which is shown in Fig. 9 for each pressure.

In Fig. 9 the curves of P_M/P_L versus k_α for the four different pressures cross in the region of $k_\alpha=0.98$ and of $P_M/P_L=0.104$. The crossing region determines the graphical solution of four simultaneous equations, based on Eq. (5) for the two unknown quantities, k_α and P_M/P_L. The final value thus determined for the ratio of M/L orbital-electron-capture probabilities in Ar^{37} decay is

$$P_M/P_L=0.104_{-0.003}{}^{+0.006}$$

and the fraction of K_α x rays in the K series of chlorine ($Z=17$) is

$$k_\alpha=0.980\pm 0.015.$$

The error limits on these quantities have been subjected to a careful detailed analysis discussed below.

EVALUATION OF EXPERIMENTAL ERRORS

One of the principal errors in this result is due to the fitting of a single-electron spectrum to the M shape. This amounts to about $\pm 2\%$. The error in establishing the zero-energy calibration of the analyzer contributes about 1.5%. The statistical uncertainty is approximately 0.5%.

The main error, however, is a systematic one. It is due to the fact that there appears to be an energy loss from the K peak. The low-energy tail from the K peak, which probably arises from degraded K events,[23,24] has been extrapolated horizontally to zero energy. The maximum contribution to the error from this procedure is unlikely to exceed about 5%. Consequently, the total error propagated quadratically in the experimental N_M/N_L values in Table I lies within $(_{-3}{}^{+5.5})\%$, and in the experimental values of N_L/N_K, within $\pm 1\%$.

A conceivable phenomenon which, if present, could cause the experimental M/L intensity ratio to appear to be too low might be Coster-Kronig transitions in the M shell,[25] with ultraviolet photon emission. By this is meant that, for example, a primary vacancy in the M_1 subshell of chlorine (binding energy $=17.5\pm 0.4$ eV[30]) might be shifted to a higher M subshell (e.g., $M_1-M_2M_3$, $M_1-M_3M_3$, or $M_1-M_2M_2$), with only a few eV of binding energy, and emission of the binding-energy difference in the form of an ultraviolet photon. Some of these ultraviolet photons could be absorbed by the quenching gas (propane) without creating an electron. Any such process would result in an M-capture event

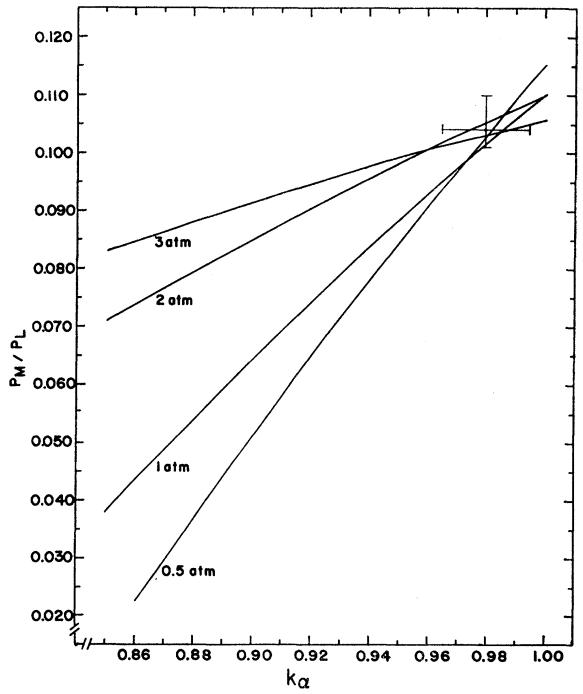

FIG. 9. Plot of P_M/P_L, the ratio of orbital-electron-capture probabilities, versus k_α, the fraction of K_α x rays in the K series of chlorine ($Z=17$). The curves represent the mean values of runs at 0.5, 1.0, 2.0, and 3.0 atm pressure (Table I).

[30] J. A. Bearden and A. F. Burr, Rev. Mod. Phys. 39, 125 (1967).

that fails to produce a single primary electron and, therefore, would not be detected.

However, this is a negligible process for the M shell at low atomic number ($Z=17$) for the following reasons. The binding energy difference (for example, in the $M_1-M_2M_3$ Coster-Kronig transition) is much more likely to appear as kinetic energy of an ejected M_2 or M_3 subshell electron in a radiationless transition. As Snell points out,[31] radiationless transitions are favored in low-Z elements and always dominate in the M, N, and higher shells for the ordinary Auger effect (e.g., $K-L-M-N$ transitions). Since Coster-Kronig transitions differ from ordinary Auger transitions only in that the vacancies are shifted within the same shell, the probability that the Coster-Kronig transition will be radiationless is essentially unity, owing to the very low transition energy.

Although the mean L-fluorescence yield of elements below $Z=23$ is unknown,[25] an extrapolation to $Z=17$ (chlorine) indicates that fewer than about 1% of L-shell vacancies in chlorine give rise to x-ray photon emission. (For the K shell of chlorine, the x-ray emission amounts to about 10% of the K vacancies.[25]) The amount of radiation in the filling of an M shell vacancy would be expected to be less than about 0.1% in chlorine. Even if the M-shell Coster-Kronig transitions were to give rise to as much as 1% of radiative transitions, which is orders of magnitude more than expected for M-shell Coster-Kronig transitions at $Z=17$, the present results would not be affected.

Consequently, in the present experiment we conclude that radiative Coster-Kronig transitions are entirely negligible.

DISCUSSION OF RESULTS

The result of the present experiments, $P_M/P_L=0.104_{-0.003}{}^{+0.006}$, has been plotted in Fig. 1, point a. Theory with exchange[3] for Ar^{37} decay predicts a value of 0.128 ± 0.0026, which is in clear disagreement with even the upper limit of the present results. In the present experiment, the upper limit on the experimental value is especially well determined. Theory without exchange[3] predicts a value of 0.0976 ± 0.001, which overlaps within the experimental error limit of the present result (Fig. 1). Curve A in Fig. 1 is based on old hydrogenlike wave functions with Slater screening,[2] and it predicts a value of about 0.034, uncorrected for exchange, which definitely is ruled out by the present results.

In spite of the apparent overlap of the present experimental result with the theoretical value of Bahcall[3] *without exchange*, any theory of M capture which fails to take account of electron-exchange–atomic-overlap effects cannot be taken rigorously, in view of the fact that for L capture the exchange correction has been thoroughly established experimentally,[27,32,33] and the predicted exchange-overlap correction $X^{M/L}$ is even larger for M capture than for L capture.[3]

The disagreement of M/L capture ratios with exchange-corrected Hartree-Fock wave-function theory[3] appears to be much larger (Fig. 1) than in the case of L/K capture ratios.[32] This suggests that the origin of these disagreements might lie with the screening assumptions made in the derivation of the Hartree-Fock wave functions of Watson and Freeman.[34]

Several new calculations of accurate analytical SCF Hartree-Fock wave functions for the low-Z region have been reported recently.[35–37] It remains to be shown whether these new Hartree-Fock wave functions, evaluated at the nucleus, will bring the theoretical L/K and M/L orbital-electron-capture ratios into closer agreement with experiment.

ACKNOWLEDGMENTS

We should like to thank Milton McLain of the Georgia Tech Reactor for irradiations of argon gas. One of us (H.G.) thanks Deutscher Akademische Austausch Dienst for a travel grant. To R. C. McFarland and J. Bruce Siberts, we are indebted for laboratory and calculational assistance in the latter stages of this investigation.

APPENDIX. Attempt to Determine the L/K Orbital-Electron-Capture Ratio in Be^7 Decay

Beryllium-7 (53.5 days) is the lowest-Z nuclide in which electron capture is known. Approximately 10% of the Be^7 decays lead to the first excited state of Li^7, which emits a prompt 478 keV γ. Following electron capture in Be^7, the daughter Li^7 atom undergoes reorganization resulting in an energy release of 55 eV from K shell vacancies and of only a few eV from L-shell vacancies.

The experimental determination of the L/K capture ratio in Be^7 decay would be of special interest, because at low Z the extrapolated correction for electron-exchange–atomic overlap[38] becomes very large.[27] The L/K capture ratio extrapolated from the theoretical results of Brysk and Rose[39] is 4.0×10^{-2}, and from the

[31] A. H. Snell, in *Alpha-, Beta-, Gamma-Spectroscopy*, edited by K. Siegbahn (North-Holland Publishing Co., Amsterdam, 1964); pp. 1545 ff.

[32] G. Winter, Ann. Physik (to be published).

[33] R. Bouchez and P. Depommier, *Proceedings of the Conference on Atomic Electrons in Nuclear Transformations* (Nuclear Energy Information Center, Warsaw, Poland, 1963), Vol. I, p. 30; and Repts. Progr. Phys. **23**, 395 (1960).

[34] R. E. Watson and A. J. Freeman, Phys. Rev. **123**, 521 (1961); **124**, 1117 (1961).

[35] G. L. Malli, Can. J. Phys. **44**, 3121 (1966); G. L. Malli and S. Fraga, *ibid.* **44**, 3131 (1966).

[36] E. Clementi, J. Chem. Phys. **38**, 1001 (1964); **41**, 295 (1964); and Tables of Atomic Functions, IBM Corp., San Jose, California, 1965 (unpublished).

[37] P. S. Bagus, Argonne National Laboratory (unpublished).

[38] J. N. Bahcall, Phys. Rev. **132**, 362 (1963); Nucl. Phys. **71**, 267 (1965); Phys. Rev. Letters **9**, 500 (1962).

[39] H. Brysk and M. E. Rose, Oak Ridge National Laboratory Report No. ORNL-1830, 1955 (unpublished); Rev. Mod. Phys. **30**, 1169 (1958).

calculations of Winter[32] is 3.32×10^{-2}. The Bahcall exchange-overlap correction[38] extrapolated to $Z=4$ is $X^{L/K}=3.74$ (see Ref. 27), so that the predicted exchange-corrected theoretical L/K capture ratio therefore is either $14.9_5\times10^{-2}$, based on Brysk and Rose,[39] or 12.4×10^{-2}, based on Winter.[32] Thus, even an approximate measurement of the experimental ratio would be of interest in testing not only the basic theories[32,39] at low atomic number, but also in testing the exchange correction, which in the case of Be^7 increases the L-capture probability by a factor of almost 4.

The source was prepared by irradiating spectroscopically pure, single-crystal flakes of beryllium metal with 30-MeV deuterons on the Berkeley 88-in. cyclotron,[40] which produced a good yield of 53.5-day Be^7 by the reaction $Be^9[(d,tn)+(d,p3n)]Be^7$. Diethylberyllium, a volatile liquid at room temperature, was synthesized[41] by the chemical reaction

$$\underset{\text{(Irradiated flakes)}}{Be^\circ} + (C_2H_5)_2Hg \xrightarrow{\Delta} (C_2H_5)_2Be + Hg^\circ$$

in a volume of less than 15 ml. Diethylmercury boils at 128°C at 1 atm pressure. About 1 to 2 ml of $(C_2H_5)_2Be$, containing radioactive Be^7, was distilled at 72°–78°C at 0.5 mm pressure, and then redistilled through a Vigreaux distillation head for final purification. The chemical reaction is very slow unless finely divided powder or flakes of beryllium are used, but very pure samples of ether-free $(C_2H_5)_2Be$ are obtained. The diethylberyllium is highly toxic, takes fire spontaneously when exposed to air, and is decomposed by moisture. It was handled at all times under a dry nitrogen or argon atmosphere.

Unfortunately, the vapor pressure of $(C_2H_5)_2Be$ is relatively low at room temperature. In order to transfer enough Be^7 activity into our proportional counter, the entire system consisting of source container and counter had to be heated to about 70°C. A higher temperature could not be used, because of decomposition of the compound. After filling the counter, the source container was removed from the system to eliminate γ background.

The initial experiments were done in glass proportional counters having metallic cathodes painted with silver on the *outside* of the glass. The glass must be sufficiently conducting at room temperature so that electric charge can penetrate through the walls to form the cathode. Soda glass has a higher electrical conductivity than borosilicate glass, and has been found to be ideal in this respect.

The final experiments with Be^7 were carried out in the aluminum counter described above for the Ar^{37} experiments. A paralysis time of 2 msec was used in these experiments, in order to avoid afterpulses, as in the Ar^{37} experiments.

In the Ar^{37} studies, the counting statistics were such that the integrated number of $M+L$ events in the sensitive volume of the counter amounted to some 6×10^4 counts in a typical run. The Be^7 experiment, however, resulted in collection of an integrated number of $L+K$ events of only some 5 000 counts, since more than 70% of the $Be^7(C_2H_5)_2$ vapor decomposed on the counter walls where it did not contribute.

The attempt to measure the L/K capture ratio in Be^7 decay in this way failed, not only because of the low counting rate, but also because the resolution of a 55-eV K event from an L event of only a few eV appears to be beyond the present state of the proportional-counter technique. Such K events do not always produce two ion-pairs, since on the average 26.5 eV in argon-propane mixtures is required to produce an ion pair, and the resolution for K events at this energy (55 eV) is some 175%.

[40] We are indebted to Prof. B. G. Harvey, Dr. J. Cerny, and Ruth Mary Larmier of the Berkeley 88-in. Cyclotron for their kindness in furnishing this irradiation.

[41] The organometallic synthesis was carried out by Professor Eugene Ashby and J. C. Carter, III; a study of the organometallic chemistry of beryllium alkyl compounds has resulted from this work and will be published elsewhere. It is not possible chemically to start with an aqueous solution of Be^7 and synthesize diethylberyllium, since hydrolysis with formation of unreactive oxychlorides results when $BeCl_2$ solutions are dehydrated; therefore, irradiation of beryllium metal was necessary and the synthesis made directly from the metal under anhydrous and inert atmosphere conditions.